

SECTOR STRUCTURE, ROTATION, AND CYCLIC EVOLUTION OF LARGE-SCALE SOLAR MAGNETIC FIELDS

E. V. IVANOV, V. N. OBRIDKO and I. V. ANANYEV
IZMIRAN, 142190, Troitsk, Moscow Region, Russia

(Received 25 January 2000; accepted 8 December 2000)

Abstract. Auto-correlation analysis was performed using digitized synoptic charts of photospheric magnetic fields for the past three solar activity cycles (1965–1994). The obtained correlograms were used to study the rotation and the zonal-sector structure of large-scale solar magnetic fields all over the observable region of heliolatitudes in various phases of solar activity. It is shown that the large-scale system of solar magnetic fields is rather complex and comprises at least three different systems. One is a global rigidly rotating system. It determines the cyclic variation of magnetic fields and is probably responsible for the behavior of magnetic fields in the polar zones. Another is a rigidly rotating 4-sector structure in the central (equatorial and mid-latitude) zone. The third is a differentially rotating system that determines the behavior of the LSSMF structure elements with a size of $\sim 30\text{--}60^\circ$ and less. This one is the most noticeable in the central zone and absent in the polar zones. Various cyclic and rotation parameters of the three field structures are discussed.

1. Introduction

Large-scale solar magnetic fields (LSSMFs) play an important role in the global organization of solar activity and formation of the heliosphere. Their structure, evolution, and rotation have been thoroughly studied during the past 30 years. The authors use either magnetograms and synoptic charts obtained from direct observations of magnetic fields (Wilcox and Howard, 1970; Stenflo, 1972, 1974, 1989, 1992; Howard and LaBonte, 1980; Snodgrass, 1983; Hoeksema and Scherrer, 1987; Makarov and Sivaraman, 1989; Antonucci, Hoeksema, and Scherrer, 1990; Howard, Harvey, and Forgach, 1990; Erofeev, 1997; Obridko and Shelting, 1997, 1998, 1999; Ananyev and Obridko, 1999), or distributions of various tracers (long-lived active features, active regions, filaments, plages, faculae, etc.) over the solar surface (McIntosh, 1972, 1992; Ivanov, 1986, 1994, 1995; Erofeev, 1999).

Both methods have their advantages and disadvantages. The former provides rich information about the rotation of magnetic fields in a broad range of heliolatitudes and heights in the solar atmosphere, but does not show their detailed structure. In the latter, the structure and evolution of large-scale magnetic fields can be studied in detail from their manifestations in the form of long-lived active features, but the study is restricted to the heliolatitude region, where these features occur, and to the periods of their maximum intensity.



Here, we have applied auto-correlation analysis to the synoptic charts of photospheric magnetic fields, digitized at a certain step in heliolatitude and heliolongitude. The method was used to study the rotation, sector, and zonal structure of large-scale magnetic fields for the past 3 activity cycles (1965–1994) in the entire heliolatitude region accessible for observation. We deal with the synodic rotation period everywhere in this work, except Figure 7, in which the sidereal angular velocity is considered to illustrate the differential rotation of the Sun.

In the second part of this paper, we discuss the experimental data and methods used for the analysis. The third part deals with the sector and zonal structure and rotation of LSSMF. The fourth part is devoted to discussion of the main results of the work.

2. Experimental Data and Methods of Analysis

Our analysis of the rotation and sector structure of large-scale solar magnetic fields is based on Stanford (Wilcox Solar Observatory) observations of the longitudinal component of photospheric magnetic fields since 1976. To extend the time interval under consideration back to 1965, we have supplemented them with the data from other two observatories: Mt. Wilson and Kitt Peak. The Stanford data cover the interval of about 19 years (1976–1994). The period from October 1964 through November 1978 (Carrington rotations (CRs) 1486–1648) is covered by photospheric synoptic maps obtained by the R. F. Howard's team at the Mt. Wilson Observatory and digitized at HAO by Stenflo (1972); the period from December 1974 through July 1984 (CR 1622–1751) is covered by the maps obtained at the Kitt Peak Observatory. All observations were brought to a single scale by comparing the overlapping data from different observatories. This gave us a continuous series of observations covering the period of 1965–1994. The synoptic maps were divided into 30 bands, evenly spaced in sine of heliolatitude. The Carrington longitudes in every band were digitized at 5° steps on Stanford maps and at 10° steps on Mt. Wilson maps. Thus, for each CR, we obtained a two-dimensional data base (72×30 points for Stanford and 36×30 points for Mt. Wilson) providing the magnetic field measurements on the solar surface. The sequence of the synoptic maps forms a time series of data from October 1964 through July 1994, digitized in heliolatitude and heliolongitude. It should be noted that the most reliable and uniform data series begins in 1976. The Mt. Wilson data from August 1965 through December 1978, digitized by Stenflo have the resolution in longitude about twice as low as the Stanford data, although it has more to do with the problem of digitizing hand drawn synoptic charts than with actual resolution of observations.

All magnetic field data for May 1976–July 1994 were divided into seven intervals, corresponding to different phases of solar cycle. To study the behavior of magnetic fields over a longer time interval (up to 10 years), we divided these data into two parts (January 1977–January 1987 and January 1987–July 1994),

corresponding to cycles 21 and 22. Later on, they were supplemented with earlier observations (September 1967–May 1976), corresponding to cycle 20.

The sector structure of large-scale magnetic fields and the rotation periods of the relevant photospheric magnetic structures were studied by means of auto-correlation analysis of a sequence of synoptic maps of photospheric magnetic fields digitized at some definite intervals in heliolatitude and heliolongitude. ACF with a shift between the data series up to 280 days were calculated for each of the 30 zones evenly spaced in sine of heliolatitude. The obtained values were plotted as correlograms. The abscissa shows the shift in days; and the ordinates, the heliolatitude in degrees.

To study the LSSMF zonal structure, we applied the correlation analysis to the series of observation data smoothed by a moving average over different time intervals (in particular, over 1 and 6 solar rotations).

The data base used to analyze the sector structure of LSSMFs in the short-period part of the time variation spectrum was obtained by subtracting the smoothed data from the corresponding original series. The analysis covered three observation intervals corresponding to solar cycles 20, 21, and 22 (September 1967–May 1976, January 1977–January 1987, and January 1987–July 1994) and 7 intervals from January 1977 through July 1994, corresponding to various phases of the solar cycle.

3. Study of LSSMF Sector Structure and Rotation

Figures 1, 3–6, and 8 illustrate the results of correlation analysis of a sequence of synoptic maps for September 1967–July 1994, digitized in heliolatitude and heliolongitude. For the smoothed short-period data series we only give the correlograms obtained by smoothing over 1 CR. The smoothing over 6 rotations virtually does not affect the result.

The correlograms in Figure 1 were obtained by correlating the synoptic maps separately for solar cycles 20, 21, and 22. The abscissa shows the shift in days; and the ordinate, the heliolatitude in degrees. The darker parts of the correlograms correspond to higher correlation.

The figures display some common features in the structure and behavior of large-scale solar magnetic fields:

(1) First of all, the central ($\varphi < \pm 55^\circ$) and polar ($\varphi > \pm 55^\circ$) zones in the correlograms differ significantly in their structure. In the central (equatorial and mid-latitude) zone, one can clearly see curved strips of maximum correlation coefficients at a shift multiple of the rotation period at the given heliolatitude (2-sector structure) and a system of less intensive straight strips corresponding to the 4-sector and the higher-order structures. In the polar zones, the sector structure is not discernible, and the correlation coefficients do not virtually change at shifts up to 280 days. So, the correlation analysis over the entire 11-year period does not reveal any sector structure in the polar zones, which implies that processes with a

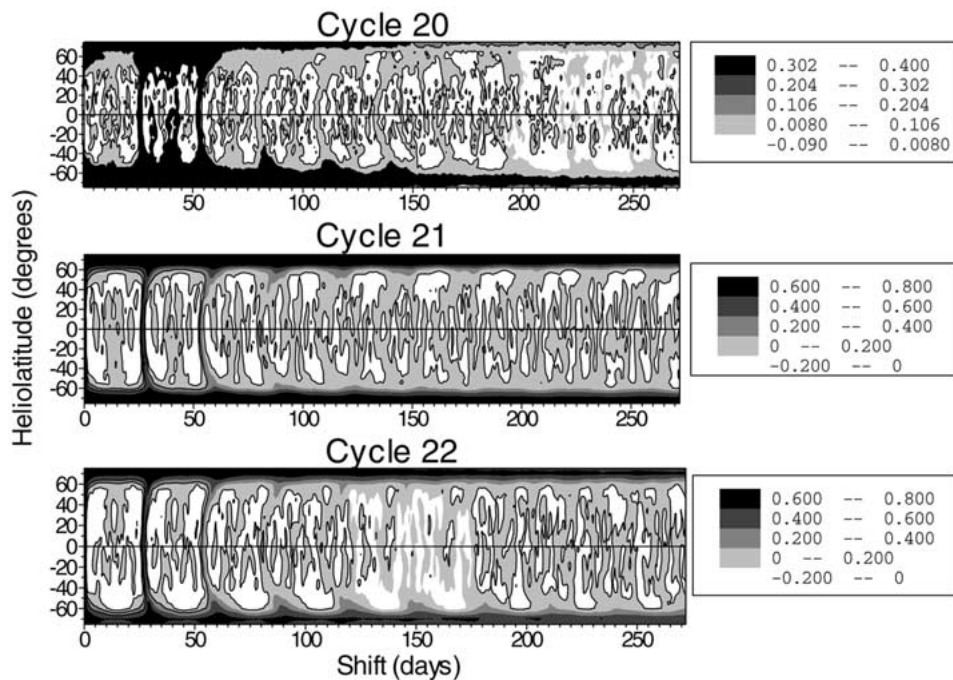


Figure 1. Correlograms of synoptic maps of the longitudinal component of the photospheric magnetic field for solar cycles 20, 21, and 22.

time scale much longer than 280 days are dominating there. Besides, it should be noted that high-latitude measurements are not too reliable.

(2) Among the modes of the sector structure, the 2-sector mode (corresponding to a shift of $\sim 27\text{--}30$ days) is the best pronounced and most extended in latitude. Its typical lifetime (or the lifetime of the corresponding structure elements) is no more than $\sim 5\text{--}6$ solar rotations. The 4-sector mode corresponding to a shift of ~ 14 days is in the second place by significance. The high-order mode corresponding to a shift of $\sim 3\text{--}5$ to ~ 12 days (with a 2–3-day interval between the modes) is the least extended in latitude and the least stable.

(3) Though changing in some detail from rotation to rotation, the sector structure conserves its general pattern for quite a long time ($>5\text{--}6$ rotations). The curved strips corresponding to the 2-sector structure reveal a noticeable differential rotation, while the straight strips corresponding to the 4-sector and the higher-order structures are indicative of a more rigid type of rotation. A similar result was reported by Ananyev and Obridko (1999). The trend from the weakly curved strips in the correlograms corresponding to the rotation of the 2-sector structure at the 27 day lag to a more curved ridge at 54, 81, or 108 days implies a significant contribution of the differentially rotating surface magnetic fields to the signal corresponding to the 2-sector structure.

In order to study the LSSMF rotation and cyclic variations in different phases of the 11-year solar cycle, we divided the observational period under consideration into the intervals covering the growth, maximum, decay and minimum phases of the solar cycle. To that end, we used the cyclic curves of the energy index of the global magnetic field $I(B_r)$, and the index of the effective solar multipole n . The indices $I(B_r)$ and n were introduced by Obridko and Ermakov (1989), Obridko and Shelting (1992), and Ivanov, Obridko, and Shelting (1997) to characterize the energy and structure of the global magnetic field of the Sun.

On a surface of radius r , $I(B_r) = \langle B^2 \rangle$, where $\langle B^2 \rangle$ is the square intensity of the magnetic field radial component averaged over the solar surface, and r is the radius of the sphere over which the field is averaged. The index was calculated by using the Stanford magnetic maps and their expansion in Legendre polynomials performed by Hoeksema (1984).

The index of the effective solar multipole is

$$n = -0.5 \log(I_{ss}/I_{ph}) / \log(2.5).$$

It is determined by taking the logarithm of the ratio of $I(B_r)$ at the source surface, I_{ss} , to its value in the photosphere, I_{ph} (Ivanov, Obridko, and Shelting, 1997). In fact, when passing from the photosphere to the source surface, the magnetic flux changes in accordance with the expression $B_{ss} = B_{ph}r^{-n}$, where $n = 3$ for a dipole source, $n = 4$ for a quadrupole source, and $n > 4$ for a higher-order multipole source. When the field under consideration is a combination of fields from several sources with different weight, n can assume values from 3 to 4 (in the case of combined dipole and quadrupole sources) or higher (in the case of a higher-order multipole field).

Figure 2 illustrates cyclic variations in $I(B_r)$ and n . Dashed lines mark out the intervals corresponding to the growth (1), maximum (2), decay (3), and minimum (4) phases of the solar cycle.

Figure 3 illustrates cyclic changes in the correlograms obtained by correlating the synoptic maps of the longitudinal magnetic field component for the time intervals corresponding to various phases of the 11-year solar cycle, i.e. the growth, maximum, decay and minimum of cycles 21 and 22. We do not give here correlograms for cycle 20 for they have low correlation coefficients. As mentioned in Section 2, the Mt. Wilson data from August 1965 to December 1978 used by us have a resolution about twice as low as the Stanford data for 1973–1993. Therefore the correlograms for cycle 20, though displaying the same regularities as those for cycles 21 and 22, are much inferior to them in clearness and informative value.

Figure 3 reveals some new regularities:

(4) In the polar zones (or in one of them), one can see the 2-sector structure to be virtually permanent and the 4-sector structure along with a slowly changing magnetic field component to appear at the growth and maximum of the cycle. According to our estimates, the latter has a characteristic time scale of about 1.5 to 2–3 years.

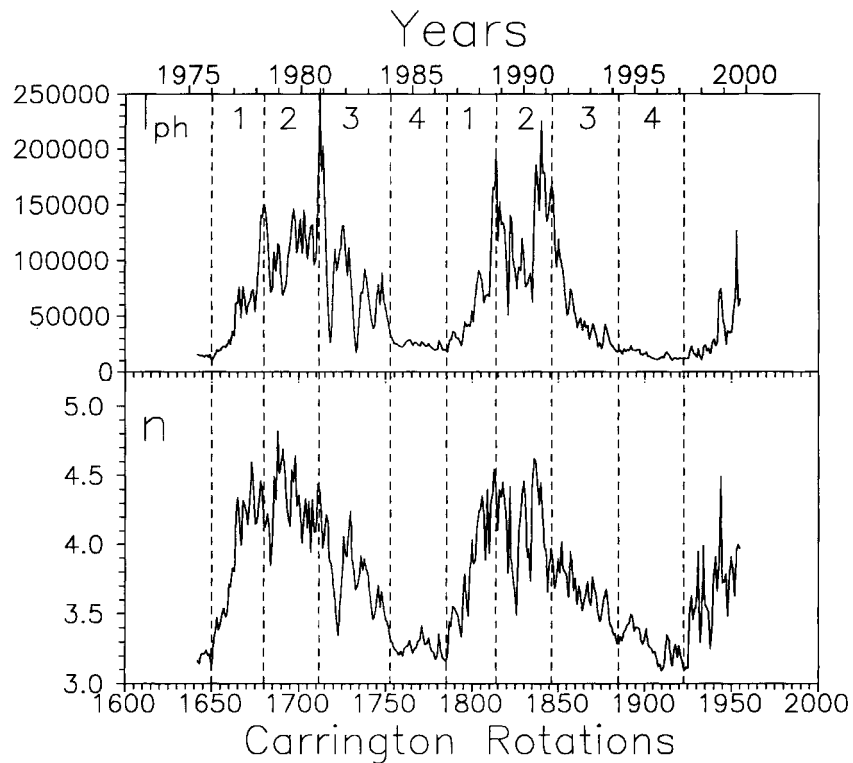


Figure 2. Cyclic variation of the energy index of the global magnetic field $I(B_r)$ and the index of the effective solar multipole n . Dashed lines mark the intervals corresponding to the growth (1), maximum (2), decay (3), and minimum (4) phases of the solar cycle.

(5) The polar and central zones are separated by the boundaries at $\varphi \simeq \pm (40-55^\circ)$. Here, the correlation coefficient displays a relative minimum compared to the lower and higher latitudes, where it is maximum. Besides the equatorial zone, relatively high correlation coefficients are also observed at heliolatitudes $\varphi \simeq \pm (60-70^\circ)$.

(6) The sector structure is most regular and stable at the decay of the 11-year cycle and exhibits the largest changes at the maximum and minimum of the cycle.

(7) In some epochs during the solar cycle, one can see a pronounced asymmetry between the northern and southern hemispheres with respect to the solar equator in the structure, rotation, and typical variation times of magnetic fields. In the central zone, the asymmetry manifests itself in the heliolatitude distribution of the sector structure and shift values in the northern and southern hemisphere; in the polar zones it manifests itself in correlation coefficients and typical variation times of the slowly changing component of the magnetic field.

Figure 4 illustrates the correlograms obtained by correlating the series of data on the magnetic field short-period component for cycles 20, 21, and 22. The short-

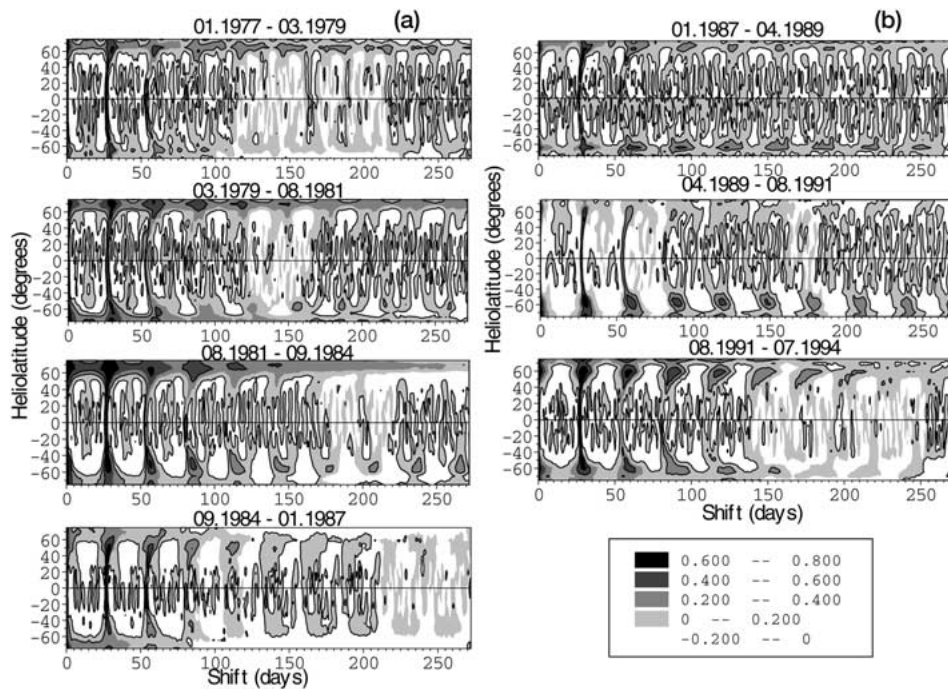


Figure 3. Correlograms of synoptic maps of the longitudinal component of the photospheric magnetic field for different phases of cycles 21 (a) and 22 (b).

period component was obtained after the data smoothed over 1 CR were subtracted from the original data series. The slowly changing component of the magnetic field is absent in the figure. At the same time, one can clearly see the 2-sector structure in the polar regions in all three cycles, and the 4-sector structure is discernible in cycle 20.

As seen from Figure 4, the type of rotation of magnetic fields differs in the polar and central zones.

(8) The rotation type changes drastically when passing from central to polar latitudes: Below $\varphi \simeq \pm 60^\circ$, the differential rotation is clearly pronounced, and the rotation period increases from ~ 27 to ~ 29 – 30 days as the heliolatitude grows; in the polar zones ($\varphi \gtrsim \pm(60$ – $65^\circ)$), the rotation period does not change with latitude (or even somewhat decreases from 30 to 29 days). The change in differential rotation is most noticeable near the maximum of the 11-year cycle. It appears as a sudden ‘jump’ of the rotation rate of magnetic fields when crossing the boundary between the central and the polar zones.

(9) The correlation coefficient for the mode that corresponds to the solar rotation period decreases from $k > 0.8$ in the first rotation to $k \simeq 0.2$ – 0.4 in the third rotation. This shows that the characteristic life-time of LSSMF features is no less than 3 solar rotations. Remember that the curved strips corresponding to the solar

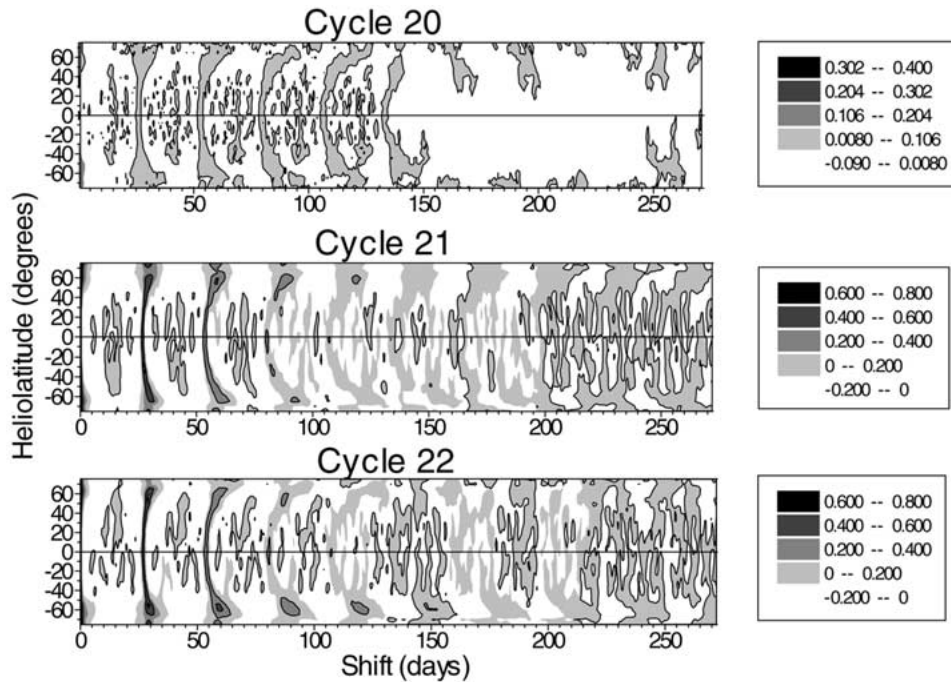


Figure 4. Correlograms of the short-period component of the photospheric magnetic field in cycles 20, 21, and 22, obtained by subtracting from the original data series the data smoothed over 1 CR.

rotation period in Figure 3 persist as a whole until their decay, as a rule, in 5–6 rotations.

(10) As we move along the curved strips corresponding to the 2-sector structure of LSSMF, the correlation coefficient grows with latitude, reaching its maximum at $\varphi \simeq \pm(45-50^\circ)$ and $\varphi \simeq \pm(60-65^\circ)$. At $\varphi \simeq \pm 55^\circ$ where a boundary is supposed to pass between the central and the polar zones, the correlation coefficient displays a relative minimum. The growth of the correlation coefficient with latitude and its relatively high values in the polar zones may probably be explained by two factors. First, the ‘noise’ component, which at lower latitudes is associated with the higher-order sector structure, is absent at $\varphi \geq \pm(45-55^\circ)$. Second, owing to the perspective shortening, the evenly spaced in sine latitude bands on the solar surface framed by the magnetograph slit extend in heliolatitude as we move to higher latitudes. Some broadening of the strips at multiples of the solar rotation period at $\varphi \simeq \pm(50-65^\circ)$ can, probably, be explained by the fact that the structure of large-scale magnetic fields in this zone is not too clearly defined (blurred or twisted boundaries strongly inclined to the meridian).

To study in more detail the sector structure and rotation characteristics of the large-scale magnetic fields in different phases of the 11-year solar cycle, we plotted correlograms for the short-period part of the magnetic field variation spectrum at shifts from 0 to 35 (Figure 5) and from 20 to 35 days (Figure 6). The figures clearly

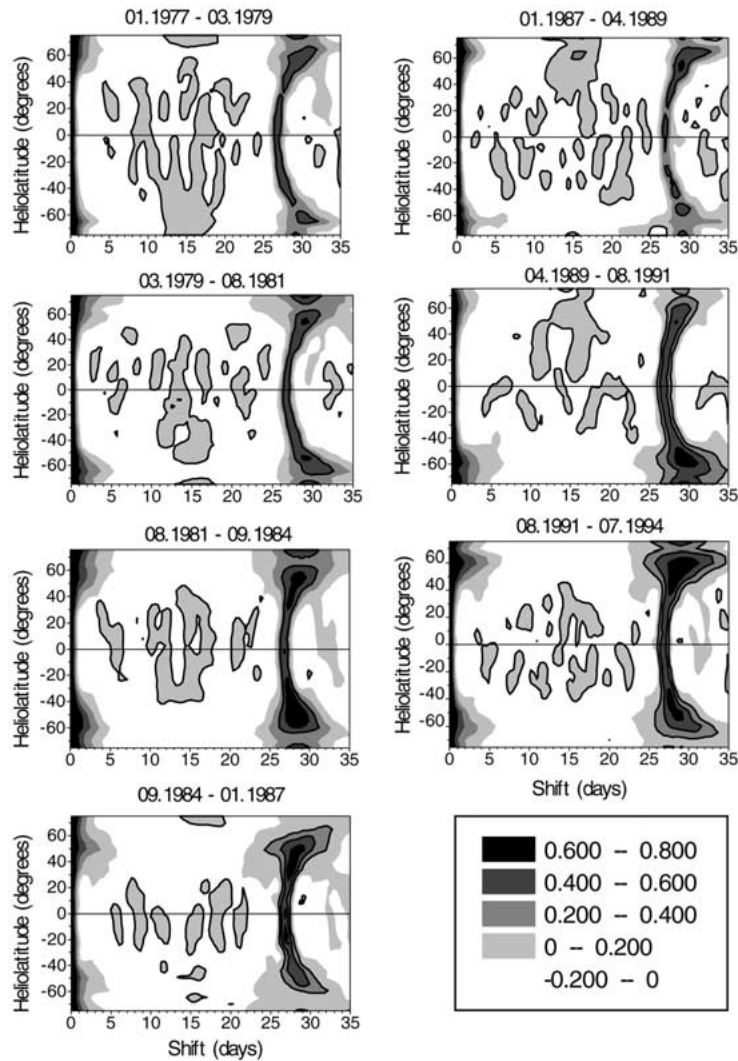


Figure 5. Correlograms of the short-period component of the photospheric magnetic field with a shift from 0 up to 35 days.

demonstrate all particular features in the structure and behavior of large-scale magnetic fields, described above: (1) the changing character of differential rotation when passing from the central zone to the poles; (2) a growth of the correlation coefficient with latitude; (3) the maximum correlation coefficient and a broadening of the strips, at a multiple of the solar rotation period, at $\varphi \simeq \pm (50-65^\circ)$, and (4) the appearance of the 4-sector structure in the polar zones in the years close to the solar minimum.

Figure 7 illustrates (a) cycle variations of the rotation rate of large-scale magnetic fields at the equator, ω_e (arc deg day $^{-1}$), and (b) variations in differential

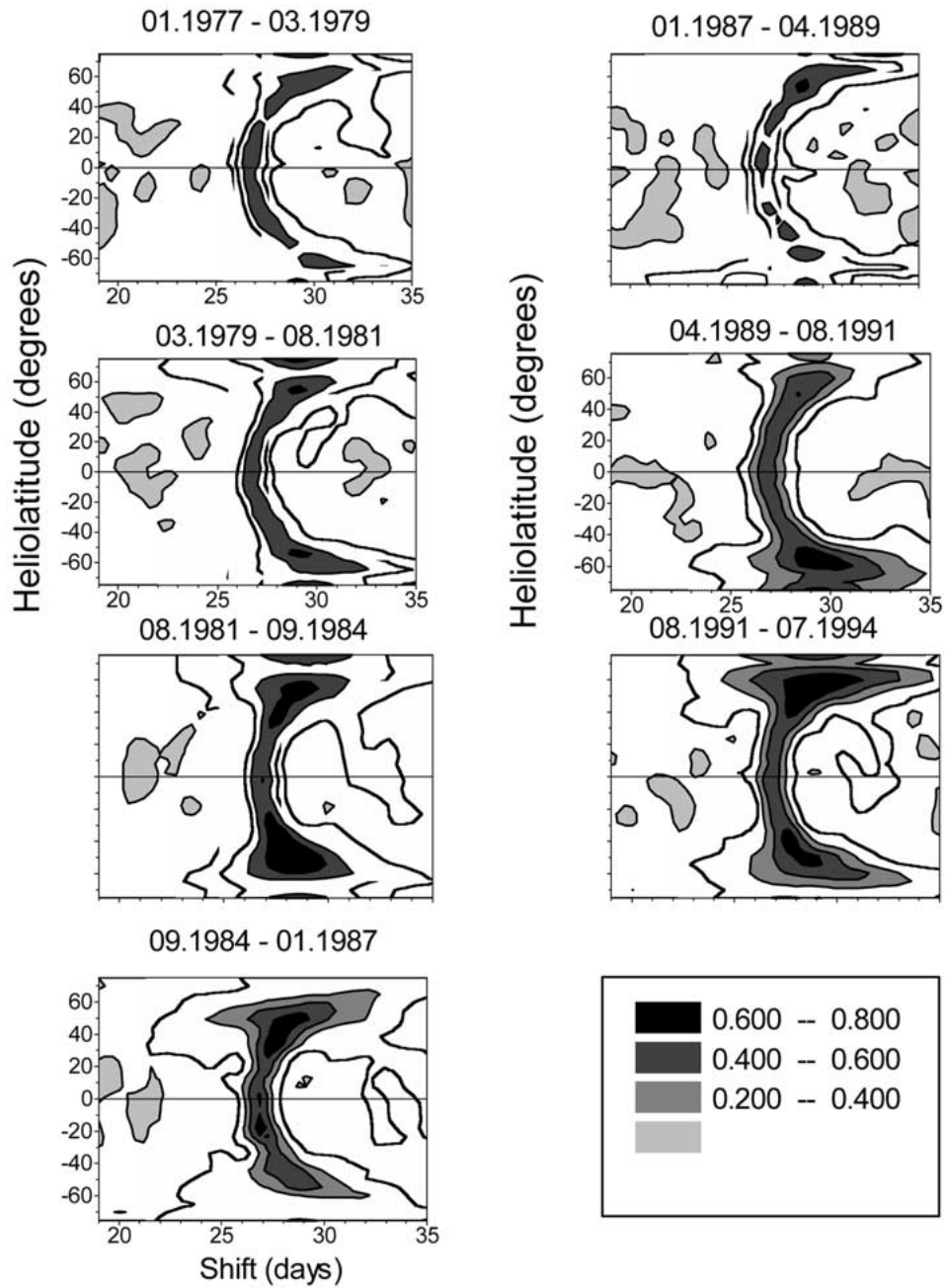


Figure 6. Correlograms of the short-period component of the photospheric magnetic field with a shift from 20 to 35 days.

rotation of the magnetic fields, b (b coefficient in the expression for differential rotation, $\omega = a - b \sin^2 \varphi$), calculated from the strips, at a multiple of the solar rotation period, on the correlograms in Figure 6. Figures 7(c) and 7(d) illustrate cycle variations of the rotation rate of large-scale magnetic fields at the equator, ω_e (arc deg day), and variations in differential rotation of the magnetic fields b calculated from the strip parts in the northern and southern hemispheres, separately. The values of ω_e and b in Figure 7 are referred to the centers of the time intervals corresponding to different phases of the 11-year cycle in Figure 6. One can readily see the rotation rate to decrease at the equator and the differential rotation to get more 'rigid' when passing from the maximum to the minimum of the cycle. Decrease of the rotation rate of magnetic fields at the equator at the minimum of the cycle does not contradict its simultaneous increase at mid and higher latitudes and is likely to be due to the generally reduced differentiability of rotation. In the minimum epoch, b is minimum and equals 1.55 (1.65 in northern and 1.45 in the southern hemisphere). It should be noted that large-scale magnetic fields rotate more rigidly than sunspots. If for sunspots, b in the expression $\omega = a - b \sin^2 \varphi$ is equal to 3.0, in our measurements, b is always close to 2, except for the growth and maximum of cycle 21 (January 1977–August 1981), when it was 2.3–2.6. It is well known that earlier observations of the photospheric gas did not reveal cycle variations in b . Note, however, that we study magnetic patterns rather than the bulk rotation; so, there is no conflict between the photospheric gas observations and the rotation of the magnetic pattern.

The properties of the 4-sector and higher-order structures and their latitudinal size depend on the phase of the 11-year cycle. The 4-sector structure is absent in the polar zones during most part of the cycle and penetrates them at the end of the growth phase and at the maximum of the cycle. The upper boundary of the zone of smaller-scale structures moves during the cycle from $\varphi \simeq \pm 45^\circ$ in the growth phase to $\varphi \simeq \pm 30^\circ$ in the decay phase and at the minimum of the cycle. This agrees with the shift of the boundary that separates the central and the polar zones (Makarov and Sivaraman, 1989; Ivanov, 1995).

Figure 8 represents the correlograms obtained by correlating the data series for different phases of cycles 21 and 22, smoothed over 1 CR. The figure reveals a zonal structure that changes with the phase of activity cycle. The common pattern is when the zones of significant auto-correlation of LSSMF variations (correlation coefficient $k \geq 0.4$) persisting for only 50–100 days, alternate with those persisting as long as >100–150 days. This corresponds to alternation of the zones of relatively fast and slow LSSMF variations. In the polar regions, the former do not appear except at the time of the solar minimum and, occasionally, near the maximum. The heliolatitude distribution of the zones of relatively fast and slow variations often displays a noticeable asymmetry with respect to the solar equator. The asymmetry changes from cycle to cycle, as well as within a cycle when passing from one phase to another. On the whole, the structure usually contains 5 more or less pronounced zones of relatively fast variations of LSSMF and 4–5 zones of

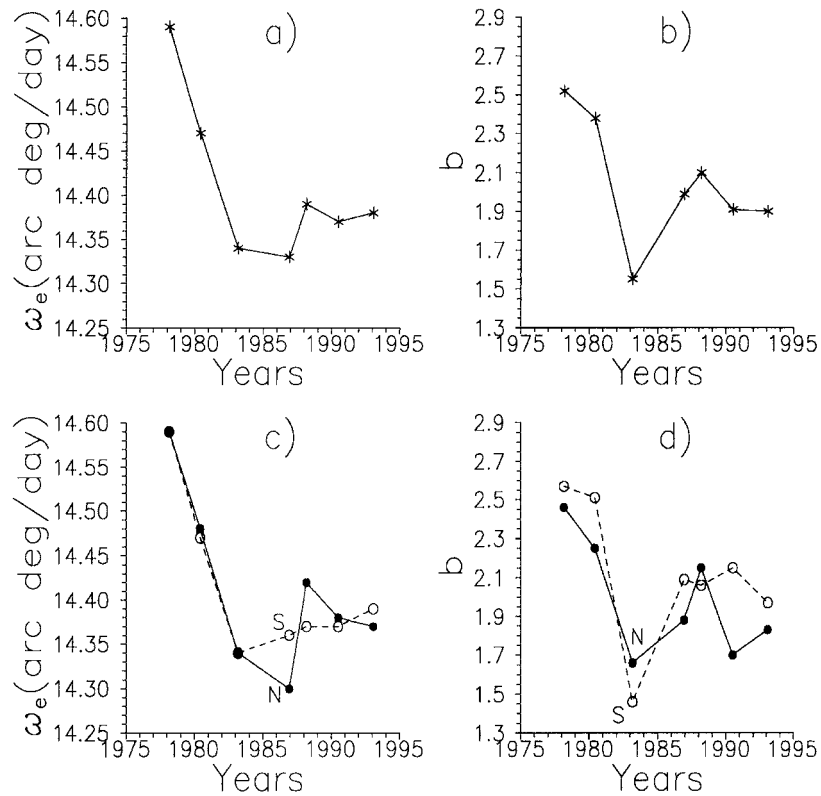


Figure 7. Cycle variations of the rotation rate of large-scale magnetic fields at the equator, ω_e (in arc deg day⁻¹) (a, c) and variations in the differential rotation of magnetic fields (b, d) (a and b – coefficients in the expression for differential rotation, $\omega = a - b \sin^2 \varphi$). (a, b) for the whole solar surface, (c, d) for the northern (N) and southern (S) hemispheres, respectively.

slower variations. The zonal structure of large-scale solar magnetic fields is dealt with in more detail in our next work.

4. Conclusions

Auto-correlation analysis of the digitized synoptic maps of photospheric magnetic fields reveals a definite zonal-sector structure and cyclic evolution of large-scale solar magnetic fields.

The sector structure comprises 2-sector, 4-sector and higher-order modes, which differ in their latitude extension and character of rotation. The 2-sector mode that corresponds to the rotation period of ~ 27 – 30 days is better pronounced and more extended in latitude than the others. The 4-sector mode, corresponding to a shift of ~ 14 days on the correlograms, is in the second place by significance. It is characterized by rigid rotation, and its extension in heliolatitude depends on the

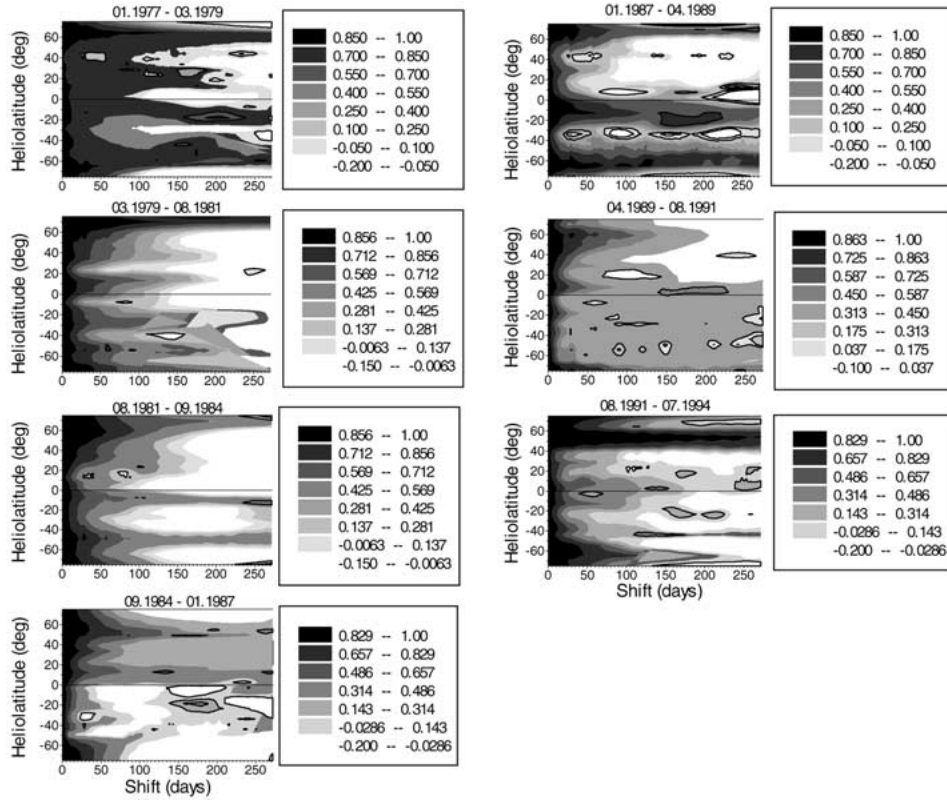


Figure 8. Correlograms of the data smoothed over 1 CR for different phases of cycles 21 and 22.

phase of the 11-year cycle. The upper boundary of the higher-order structures moves from $\varphi \simeq 45^\circ$ in the growth phase to $\varphi \simeq 30^\circ$ at the minimum of the cycle in full agreement with the latitude shift of the neutral line that separates the magnetic fields of the central and polar zones. The sector structure is most regular at the decay of the cycle. Though changing in detail, it retains its main features over quite a long time interval (up to ~ 6 solar rotations and longer).

The rotation of the 2-sector structure changes drastically when passing from central to polar latitudes. Below $\varphi \simeq \pm 55^\circ$, the differential rotation is clearly pronounced, and the rotation period increases from ~ 27 to ~ 29 – 30 days as the helioaltitude grows. In the polar zones ($\varphi \gtrsim \pm 55^\circ$), the rotation period does not change (or even somewhat decreases from 30 to 29 days) with the growth of latitude. The changing character of differential rotation is most noticeable near the minimum of the 11-year cycle.

In the central (equatorial and mid-latitude) zone, the magnetic field variations with a period of ≤ 1 rotation determined by the 2-sector, 4-sector and higher-order LSSMF structure are basic. In the polar zones, much slower variations with a period more than 280 days (and, in our estimate, probably even more than 3 years) pre-

dominate. The latter are due to long-time cyclic variations of LSSMF. The 2-sector mode in the polar zones can only be revealed when periods shorter than 3 years are analyzed and exists virtually in all the phases of the solar cycle. It implies that the Sun looks like a tilted dipole virtually throughout the cycle. The 4-sector structure is not noticeable except in the years close to the solar maximum. Its appearance coincides in time with the fast drift of equatorial magnetic fields towards the poles.

Large-scale magnetic fields always display more rigid rotation than sunspots. The rotation rate of LSSMF at the equator decreases and at the mid- and higher latitudes, increases when passing from the maximum to the minimum of the cycle. At the same time, the differential rotation gets more 'rigid'.

The correlograms based on the data series smoothed over 1 CR display a more complex zonal structure, than simple division into the central and polar zones with changes depending on the phase of the solar cycle. Most frequently we observe a pattern where the latitude zones of relatively fast LSSMF variations alternate with the zones of slower variations. The former appear in the polar regions at the minimum and, occasionally, in the years near the maximum of the solar cycle. A typical zonal structure comprises 9–10 zones, of which 5 are the zones of relatively fast LSSMF variations (< 50 – 100 days) and the other 4 or 5 are the zones of slower variations (> 100 – 150 days).

A noticeable asymmetry with respect to the equator is observed both in the zonal, and in the sector structure of large-scale solar magnetic fields. The asymmetry changes from cycle to cycle, as well as with the phase of the activity cycle.

Thus, the large-scale solar magnetic field system is rather complex. It involves at least three different systems. One is the global rigidly rotating system that determines the cyclic variation of magnetic fields. It is the system that, probably, determines the behavior of magnetic fields in the polar zones. Another is the rigidly-rotating 4-sector structure system in the central (equatorial and mid-latitude) zone. Both systems are likely to correspond, on the one hand, to the rigidly rotating deeplying magnetic fields and, on the other, to the open magnetic fields, which form the heliospheric current sheet and the heliosphere as a whole. The third system is the differentially rotating system of surface magnetic fields, which determines the behavior of the LSSMF structure elements with a size of ~ 30 – 60° and less and corresponds to closed magnetic fields. It is best pronounced in the central zone and is absent in the polar zones.

The nature of the LSSMF zonal structure (both central-polar and 9-zonal) is so far not clear enough, and we are going to continue its study in our future works.

Acknowledgements

The work was supported by the Russian Foundation for Basic Research (Projects N 98-02-16189 and 99-02-18346) and the National Program for Astronomy.

References

- Ananyev, I. V. and Obridko, V. N.: 1999, *Astron. Rep.* **43**, 831.
- Antonucci, E., Hoeksema, J. T., and Scherrer, P. H.: 1990, *Astrophys. J.* **360**, 296.
- Erofeev, D. V.: 1997, *Solar Phys.* **175**, 45.
- Erofeev, D. V.: 1999, *Solar Phys.* **186**, 431.
- Hoeksema, J. T. and Scherrer P. H.: 1987, *Astrophys. J.* **318**, 428.
- Howard, R. and LaBonte, B. J.: 1980, *Astrophys. J.* **239**, L33.
- Howard, R., Harvey, J. W., and Forgach S.: 1990, *Solar Phys.* **130**, 295.
- Ivanov, E. V.: 1986, *Soln. Dann.* No. 7, 61.
- Ivanov, E. V.: 1994, in D. N. Baker, V. O. Papatashvili and M. J. Teague (eds.), 'Solar Terrestrial Energy Program, The Initial Results from STEP Facilities and Theory Campaigns', *Proc. STEP Symp./5th COSPAR Colloq., COSPAR Colloquia Series 5*, p. 133.
- Ivanov, E. V.: 1995, *Bull. Russian Acad. Sci. Phys.* **59**, 1133.
- Ivanov, E. V., Obridko, V. N., and Shelting, B. D.: 1997, *Astron. Rep.* **41**, 236.
- Makarov, V. I. and Sivaraman, K. R.: 1989, *Solar Phys.* **123**, 367.
- McIntosh, P. S.: 1972, *Rev. Geophys. and Space Phys.* **10**, 837.
- McIntosh, P. S., 1992, in: M. Summerfeld (ed.), *Solar Activity Observations and Predictions Progress in Astronautics and Aeronautics*, Academic Press, New York, p. 65.
- Obridko, V. N. and Ermakov, F. A.: 1989, *Astron. Circ.* 1539, 24.
- Obridko, V. N. and Shelting, B. D.: 1992, *Solar Phys.* **137**, 167.
- Obridko, V. N. and Shelting, B. D.: 1997, in: V. I., Makarov and V. N., Obridko (eds.), *Present-day Problems of Solar Cycles*, St.-Petersburg: GAO, p. 193.
- Obridko, V. N. and Shelting, B. D.: 1998, in: V. I. Makarov, and V. N. Obridko (eds.), *New Cycle of Solar Activity: Observations and Theory*, GAO, St.-Petersburg, p. 137.
- Obridko, V. N. and Shelting, B. D.: 1999, *Solar Phys.* **184**, 187.
- Obridko, V. N. and Shelting, B. D.: 2000, *Astron. Zh.* **77**, 124.
- Obridko, V. N. and Shelting, B. D.: 2000, *Astron. Zh.* **77**, 303.
- Snodgrass, H. B.: 1983, *Astrophys. J.* **270**, 288.
- Stenflo, J. O.: 1972, *Solar Phys.* **23**, 307.
- Stenflo, J. O.: 1974, *Solar Phys.* **36**, 495.
- Stenflo, J. O.: 1989, *Astron. Astrophys.* **210**, 403.
- Stenflo, J. O.: 1992, in K. L. Harvey (ed.), *Proceedings of the National Solar Observatory Sacramento Peak 12th Summer Workshop*, San Francisco, California, p. 421.
- Wilcox, J. M. and Howard, R. F.: 1970, *Solar Phys.* **13**, 251.
- Wilcox, J. M., Schatten, K. H., Tanenbaum, A. S., and Howard, R.: 1970, *Solar Phys.* **14**, 255.